Chinese Herbal Medicines 11 (2019) 379–386

Contents lists available at ScienceDirect

Chinese Herbal Medicines

journal homepage: www.elsevier.com/locate/chmed

Original Article

Selection of quality markers of *Jasminum amplexicaule* based on its anti-diarrheal and anti-inflammatory activities: Effect-target affiliation-traceability-pharmacokinetics strategy

Ai-li Xu[a,b,c,d], Bu-ming Liu[e], Dong-mei Sun[b,c,d], Xiao-li Bi[b,c,d], Da-ke Cai[b,c,d], Zhao Chen[b,c,d], Xue-jun Huang[b,c,d], Jie-yi Jiang[b,c,d], Ping Ding[a,*]

[a] *School of Traditional Chinese Medicine, Guangzhou University of Chinese Medicine, Guangzhou 510006, China*
[b] *Guangdong Province Engineering Technology Research Institute of TCM, Guangzhou 510095, China*
[c] *Guangdong Second TCM Hospital, Guangzhou University of Chinese Medicine, Guangzhou 510095, China*
[d] *Guangdong Provincial Key Laboratory of Research and Development in Traditional Chinese Medicine, Guangzhou 510095, China*
[e] *Guangxi Key Laboratory for TCM Quality Control Research, Guangxi Institute of Chinese Medicine and Pharmaceutical Science, Nanning 530001, China*

ARTICLE INFO

Article history:
Received 10 October 2018
Revised 22 April 2019
Accepted 6 May 2019
Available online 18 August 2019

Keywords:
isochlorogenic acid B
Jasminum amplexicaule
Buch.-Ham. (Oleaceae)
methyl caffeate
NF-κB
pharmacokinetics
quality markers

ABSTRACT

Objective: To investigate therapeutic mechanism in *Jasminum amplexicaule* (Oleaceae) and verify its main active component as quality control markers

Methods: Established mouse models of diarrhea, intestinal angina, and inflammation were firstly used to select herb fractions with optimum efficacy, followed by an *in vitro* experiment to determine key targets associated with effects of *J. amplexicaule* extract. The selected fractions were isolated and purified, its components were identified, and the obtained compounds were verified for their effects on NF-κB and iNOS. Finally, effective compounds were administered to rats, their plasma pharmacokinetic parameters were calculated, and quality markers (QMs) reflecting therapeutic activities of *J. amplexicaule* were confirmed.

Results: Trichloromethane and ethyl acetate fractions had significant anti-diarrheal, anti-inflammatory, and analgesic effects. The trichloromethane fraction also reduced BDNF, p38 MAPK, p-p38 MAPK, NF-κB p65, and p-NF-κB p65 levels in the ileum in a rhubarb-induced diarrhea mouse model. Additionally, it inhibited LPS-induced NF-κB transcription and nitric oxide (NO) production in RAW264.7 macrophages, which suppressed iNOS expression. Therefore, the trichloromethane fraction was further investigated. QMs candidate selection identified 17 compounds, and results of *in-vitro* therapeutic validation indicated that methyl caffeate and isochlorogenic acid B had the strongest anti-diarrheal, anti-inflammatory, and analgesic activities. After being validated by a UHPLC–MS-MS method, concentrations of these target compounds were accurately determined in the rat plasma and pharmacokinetic parameters were calculated. C_{max}, t_{max}, and $t_{1/2}$ were respectively 575.35 ng/mL (2.963 nmol/mL), 0.5 h, and 0.45 h for methyl caffeate and 262.03 ng/mL (0.5034 nmol/mL), 0.25 h, and 2.03 h for isochlorogenic acid B. Because these candidate compounds exhibited favorable pharmacokinetics, they were considered as QMs of *J. amplexicaule*.

Conclusions: The present study accurately and effectively identified QMs of *J. amplexicaule* that act as indicators of efficacy and quality.

1. Introduction

Jasminum amplexicaule Buch.-Ham. (Oleaceae) Wild is widely distributed in Guangdong, Guangxi, and Hainan provinces of China. Dried stems and leaves of this herb clear away the heat evil, expel superficial evils, and relieve dampness and stagnation. Pharmacology researches have also shown that *J. amplexicaule* cures diarrhea, enterogastritis, dysentery, and stomachache (Gao, Yin, & Xie, 2014; Jia, Su, & Peng, 2008; Tanahashi, Shimada, & Nagakura, 1992). However, related pharmacology research only included its efficacy of the whole herb or certain extract (Gao et al., 2014; Jia et al., 2008; Tanahashi, Takenaka, & Nagakura, 1995, 1999, 2000),

* Corresponding author.
E-mail address: dingpinggz@126.com (P. Ding).

https://doi.org/10.1016/j.chmed.2019.08.002
1674-6384/

lacking the comprehensive evidence chain of its mechanism and exact compounds bearing such activities (Liu, Cheng, & Guo, 2017; Shi, Song, & Li, 2014; Wang, Wang, & Wang, 2017; Yang, Zhang, & Wu, 2017).

A possible solution to this problem is integrating scattered investigation and evaluation. Compounds found in the *J. amplexicaule* extract should not only be evaluated by their own efficacy on the key therapeutic target (Fredericksen, Villalba, & Olavarría, 2016; Jahromi, Jamshidi, & Farazmand, 2017; Umamaheswari, Asokkumar, & Rathidevi, 2007; Wang, Chen, & Du, 2015; Zhang, Wang, & Sha, 2012), but also experience content determination to validate their capability of fulfilling dose-effect relation (Delporte, Backhouse, & Erazo, 2005; Gupta, Mazumder, & Sambath, 2005; Gálvez, Crespo, & Jiménez, 1993; Uddin, Shilpi, & Alam, 2005); Finally, compounds selection would be analyzed for the pharmacokinetic parameters that indicate their bioavailability in the body (Li, Fan, & Wang, 2015; Li, Zhai, & Jiang, 2015; Shi, Zheng, & Liu, 2015; Wan, Sun, & Yu, 2013).

2. Methods and materials

2.1. Chemicals and reagents

The following 17 compounds were used for activity and target affiliation tests: Salicylic acid (purity 98%), ferulic acid (purity 98%), and protocatechuic acid (purity 98%) were purchased from the National Institutes for Food and Drug Control (Beijing, China); 3-hydroxy-4-methoxybenzoic acid (purity 90%), methyl caffeate (purity 90%), 5-hydroxy-3,5-dimethoxybenzoic acid (90% purity), and indole-3-carboxaldehyde (90% purity) were purchased from J&K Scientific Ltd. (Guangzhou, China); Scopoletine (90% purity), caffeic acid (90% purity), and isochlorogenic acid A (90% purity) were purchased from Chengdu Herbpurify Co., Ltd. (Chengdu, China); Caffeine (90% purity), protocatechuic acid methyl ester (90% purity), 4-hydroxy-4-(3-hydroxy-1-butenyl)-3,5,5-trimethyl-2-cyclohexen-1-one (90% purity), isochlorogenic acid B (90% purity), and 3,5-*O*-dicaffeic quinine acid methyl ester were self-isolated using preparative HPLC (because these compounds were not purchasable). HPLC grade reagents for pharmacology study, mechanism evaluation, component screening, cytobiology, and pharmacokinetics research, such as dimethyl sulfoxide, tris(hydroxymethyl)aminomethane, methanol, and acetonitrile, were purchased from Sigma Aldrich (Darmstadt, Germany); MTT was also purchased from Sigma Aldrich. For extraction and purification, analytical grade reagents used were purchased from Guangzhou Chemical reagent Co., Ltd. (Guangzhou, China). Deionized water was self-prepared using a Millipore system (Darmstadt, Germany).

As positive controls, berberine hydrochloride tablet (Huanan Pharmaceutical Co., Ltd., Dongguan, Guangdong, China), paracetamol tablet (Sinopharm Shantou Jinshi Pharmaceutical Co., Ltd., Shantou, Guangdong, China), indomethacin tablet (Huanan Pharmaceutical Co. Ltd.), and neostigmine injectable solution (Ange Pharmaceutical Co., Ltd., Nanjing, Jiangsu, China) were used.

2.2. Instruments

All absorbance measurements were carried out by Varioskan Flash spectral scanning digital reader (Thermo-Fisher Scientific, San Jose, CA, USA). NF-κB transcription was determined by Varioskan Flash ELISA (Thermo-Fisher Scientific). For western blotting and other related cytobiology experiments, the main instruments used were an inverted fluorescence microscope (Leica Microsystem, Buffalo Grove, IL, USA), a 37 °C CO_2 incubator (Thermo-Fisher Scientific), Tanon 5200 Multi imaging system (Tian Neng Technology Co., Ltd., Shanghai, China), IQ^{TM}5 fluorescence quantitative PCR (Bio-Rad, Hercules, CA, USA), SmartSpec plus nucleic acid protein analyzer (Bio-Rad), and PowerPac Basic electrophoresis system (Bio-Rad). The extract fractions were injected into a Shimadzu LC-6AD semi-preparative HPLC (Shimadzu, Kyoto, Japan) using a Welch Ultimate XB-C18 column (250 mm × 10 mm, 10 μm) to obtain pure compounds, and the resulting samples were analyzed by a Varian INOVA 500NB NMR instrument for the identification of chemical structures. For the determination of target compounds, *J. amplexicaule* extracts were injected to a Thermo TSQ Quantum MS (Thermo-Fisher Scientific) with electrospray ionization. For the pharmacokinetics study, pretreated rat plasma samples were also analyzed by the same instrument as that of extract.

2.3. Evaluation and selection of extraction parts

The dried herb of *J. amplexicaule* Buch.-Ham. (Oleaceae) (Bergium) Wild was soaked by methanol for five cycles (7 d per cycle), the obtained crude extract was concentrated and further extracted by petroleum ether, acetic ether, trichloromethane and *n*-butanol. The rhubarb induced diarrhea mice model (NIH mice) was given a dosage of each fraction equivalent to 3.900 g/kg and 0.975 g/kg (high dose and low dose) of crude drug, and ileum tissue was taken after sacrificing the mice.

For Western-blotting, 100 mg of the obtained tissue was grounded with liquid nitrogen and prepared with 1 mL RIPA solution containing PMSF. Then, the solution was centrifuged and the supernatant was electrotransferred to a PVDF membrane. Nonspecific binding was blocked by 5% non-fat milk. Subsequently, the membrane was incubated by the primary antibody: β-actin, goat anti-rabbit IgG H&L (HRP), BDNF, p38 MAPK, NF-κB p65, p-p38 MAPK, overnight at 4 °C. The membrane was wash by TBST twice for 10 min, followed by incubation of secondary antibody: goat anti rabbit IgG-HRP (1:2000 in TSBT) in shake table for 1 h. The obtained membrane was wash by TBST four times for 5 min. After the above-mentioned steps, the membrane was imaged by ECL, the fluorescence absorbance was determined by Varioskan Flash and the results were analyzed by SPSS17.0 and GraphPad Prism 5 (GraphPad, San Diego, CA, USA).

An RT-PCR method was used for quantitative determination of iNOS mRNA expression of each fraction. RAW264.7 cell cultivated in DMEM medium was added with LPS, Dexamethasone (as positive control), and *J. amplexicaule* fractions. After incubation for 24 h, the medium was disposed, with PBS washing (1 mL per well) for three times, then stored in 1 mL TRIzol at −80 °C. RevertAid^{TM} First Strand cDNA Synthesis Kit was used for the transcription of mRNA to cDNA (Thermo-Fisher Scientific, San Jose, CA, USA), the procedure and sequence was as followed: total RNA was extracted from RAW264.7 cell, and added with 1 μL of Oligo$(dT)_{18}$ and ddH_2O to 12 μL, the solutin was placed in 70 °C for 5 min and immediately transferred to ice water for 2 min; then, 4 μL of reaction buffer (5 times diluted), 1 μL of RiboLock^{TM} Rnase Inhibitor (20 U/μL), 2 μL of 10 mmol/L dNTP Mix, 1 μL of RevertAid^{TM} M-MuLV Reverse was subsequently added and diluted by Transcriptase (200 U/μL) to the total volume of 20 μL. The obtained cDNA was amplified by a primer designed using Primer 6.0 software, the sequences was F (5′-3′): ACGGCTACCACATCC and R (5′-3′): CAGACTTGCCCTCCA for 18 s (162 bp), for iNOS it was F(5′-3′): CCCAAGGTCTACGTTCAGGAC and R(5′-3′):GGAAAAGACTGCACCGAAGATATCT (246 bp); The prepared solution (1 μL) was placed in PCR instrument, and added with 12.5 μL of Maxima^{TM} SYBR Green/Fluorescein, primer solution (both 1 μL), qPCR MasterMix (2X), 9.5 μL ddH_2O. Following a 94 °C × 30 s→55 °C × 30 s→72 °C × 50 s (45 cycles) and 72 °C × 7 min programs. Finally, the obtained results were analyzed and the suitable fraction was selected.

2.4. Selection of main active compounds

According to the evaluation result of extraction parts, compounds in the trichloromethane (with optimum performance) was isolated, and then identified by NMR for their own chemical structures; All compounds isolated were weighed and calculated for their own proportion. At the same time, each of those compounds were tested in LPS induced RAW 264.7 cell for their own NF-κB inhibition and iNOs emission activities: pNF-κB-Luc transferred RAW 264.7 cell was planted in a 96 well plate, then processed with the method described in Section 2.3, and subsequently analyzed by GraphPad Prism 5.01, and candidate compounds with good potential were chosen.

2.5. Determination of selected compounds

The content of the candidate compounds were determined by LC–MS-MS method as followed: Agilent Eclipse SB-C_{18} (2.1 mm × 100 mm, 1.7 μm) column (Agilent Technologies) with a mobile phase containing acetonitrile and deionized water with 0.1% formic acid at a flow rate of 0.3 mL/min; The injection volume was 10 μL. Mass spectrometry conditions were as follows: The ion source was electrospray ionization, and detection mode was selective reaction monitoring in both positive and negative ion modes. The spray voltage was 3500 V (3000 V for negative ion mode), vaporization temperature was 350 °C, capillary temperature was 300 °C, sheath gas pressure was 30 psi, auxiliary gas pressure was 10 psi, tube length offset was −105 V, and skimmer offset was 5 V. Ion pair of Methyl caffeate was 193/133.5(*m/z*), 517/163(*m/z*) of isochlorogenic acid B, and 286/201 of piperine (IS), with 20, 25 and 22 V of collision energies, respectively. Concentrations of the target compounds were calculated, and the representative chromatogram was shown in Fig. 5.

2.6. Pharmacokinetic research

For the pharmacokinetics experiment, six SD rats [three male and three female, weighing (230 ± 20) g] were procured from the Guangdong experimental animal center (Guangzhou, China). The animal welfare and experimental procedures (including that of the mice) were strictly in accordance with the guide for the care and use of laboratory animals and the related ethical regulations of the Guangdong Province Engineering Technology Research Institute of TCM. The rats were fasted overnight and an inflammatory model was established using a previously reported method (Gao et al., 2014; Jia et al., 2008). The rats were administered 30.4 mg/kg of trichloromethane extract, and 200 μL of blood was withdrawn from the left common carotid artery at time points of 0.083 (5 min), 0.167 (10 min), 0.25 (15 min), 0.333 (20 min), 0.5, 1, 2, 3, 4, 6, 8, and 24 h. The obtained blood samples were then centrifuged (4 °C, 8000 r/min) to separate the plasma, and heparin was added to the plasma before the samples were stored at −20 °C.

2.7. Pretreatment of plasma samples

Spiked or test plasma samples (100 μL) obtained as described in Section 2.8, were transferred to 1.5-mL centrifuge tubes, and 10 μL of internal standard (piperine, 1 μg/mL) and 400 μL of methyl *t*-butyl ether were added. After vortex-mixing for 3 min, 300 μL of supernatants were transferred to clean tubes and dried under nitrogen stream; The residues were re-dissolved in methanol and centrifuged (4 °C, 13 000 r/min) for 5 min. Finally, 80 μL of the supernatants were transferred to injection vials ready for analysis.

2.8. Analysis of pharmacokinetic parameters

Plasma samples (prepared by the procedure described in Section 2.6) were injected into the LC–MS-MS instrument and analyzed using the established method (Section 2.5). The obtained TIC chromatograms were recorded, and peak areas for each of the specified compounds were calculated by LC-Quan software (Thermo-Fisher Scientific). Further, concentrations of the target compounds were determined by the Biological Availability Processing Program 2.0 (BAPP2.0, China Pharmaceutical University, Nanjing, China) to calculate pharmacokinetic parameters.

3. Results and discussion

3.1. Evaluation of fractions

As shown in Fig. 1 and Table 1, although petroleum ether, acetic ether, *n*-butanol and methanol fractions showed significant inhibition in all targets tested, the above-mentioned fractions had no dose-dependent influence on iNOS protein expression, which means such fractions may not be suitable for further research. However, on the other hand, the trichloromethane fraction performed much better in both activity and dosage, as well as all targets mentioned above, indicating that the active compounds in *J. amplexicaule* mainly concentrated in this fraction. Furthermore, the effect of down-regulating protein expression was far more obvious in NF-κB, which could explain their ability to regulate multiple inflammatory factors. As a conjunction of various pathways, NF-κB activation results in the expression and regulation of factors, such as IL-1, IL-6, IL-8, TNF-α, and iNOS, all of which are closely related to inflammatory enteritis. Thus, the transcription activity of NF-κB influenced by the trichloromethane fraction was determined using the luciferase method. As shown in Fig. 1, the inhibition of the above mentioned fractions had significant difference comparing with model group in the nontoxic concentration range (25–100 μg/mL), indicating that *J. amplexicaule* effectively inhibited NF-κB transcription. Similar results were found for both iNOS mRNA expression (Table 2) and NO production in the culture supernatants of RAW264.7 cells. iNOS mRNA expression was determined by RT-qPCR, and the trichloromethane fraction (in the same concentration range as that of NF-κB) significantly downregulated the expression of iNOS mRNA. NO production was also inhibited by the trichloromethane fraction as analyzed by the Griess method.

3.2. Identification and validation of compounds in trichloromethane fraction

Isolated and purified solutions containing individual compounds (confirmed by HPLC analysis) were analyzed by NMR to

Table 1
Effect of each fraction of *J. amplexicaule* on relative expression of possible target of NF-κB (mean ± SD, $n = 3$).

No.	Compounds	Relative expression of NF-κB p65
1	Blank	1.00 ± 0.00
2	Model	6.86 ± 0.22
3	Berberine (positive control)	3.67 ± 0.32
4	Petroleum ether (low dose)	6.86 ± 0.52
5	Petroleum ether (high dose)	6.49 ± 0.68
6	Trichloromethane (low dose)	3.23 ± 0.33
7	Trichloromethane (high dose)	3.65 ± 0.35
8	Acetic ether (low dose)	2.53 ± 0.25
9	Acetic ether (high dose)	3.94 ± 0.27
10	*n*-butanol (low dose)	4.65 ± 0.40
11	*n*-butanol (high dose)	6.73 ± 0.75
12	Methanol (low dose)	3.38 ± 0.46
13	Methanol (high dose)	2.61 ± 0.23

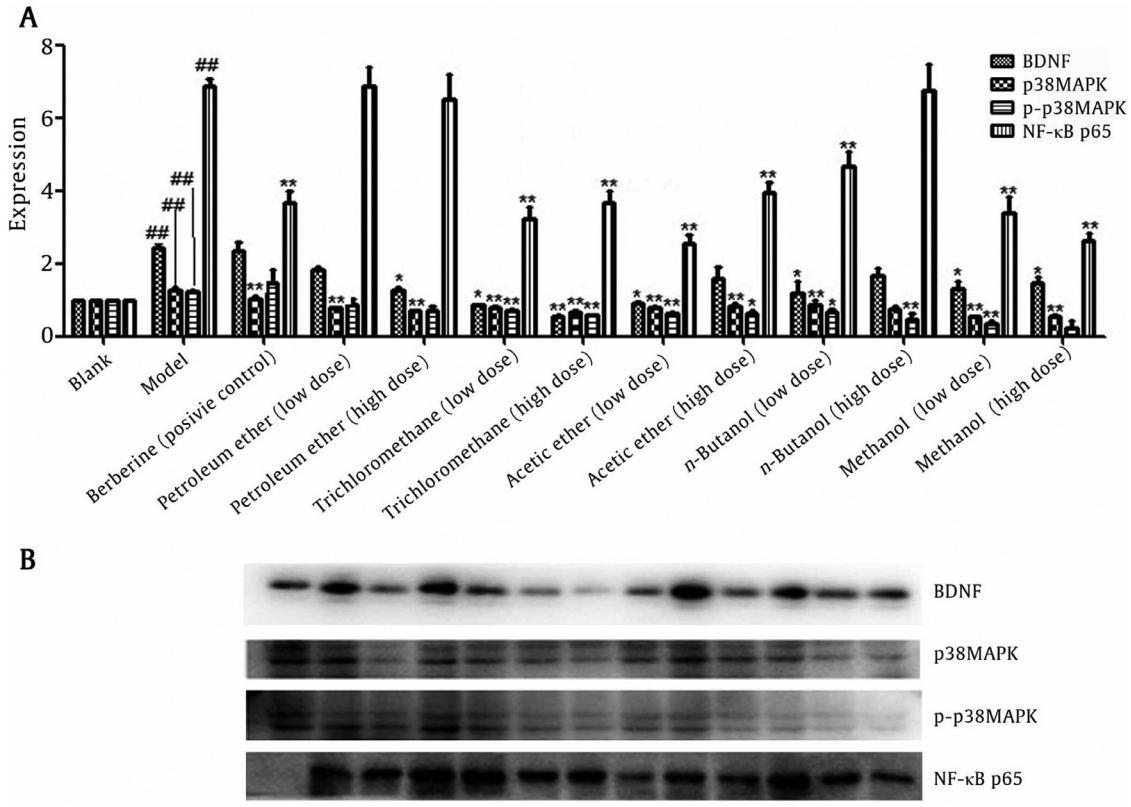

Fig. 1. Effect of each fraction on protein expression of possible targets (A); Western blot image of inhibition activity of different fractions on each target (B).

Table 2
Effect of each fraction of *J. amplexicaule* on iNOS mRNA relative expression (mean ± SD, $n = 3$).

Groups	Concentration / (μg·mL^{-1})	Relative expression
Control	–	1.00 ± 0.30
Model (LPS)	0.5	8.81 ± 0.02$^{\#\#}$
Dexamethasone	0.5	5.66 ± 0.13**
Trichloromethane	12.5	0.53 ± 0.004**
	25	0.03 ± 0.002**
	50	0.01 ± 0.0003**
Acetic ether	12.5	2.38 ± 0.12**
	25	0.15 ± 0.004**
	50	0.01 ± 0.001**
n-butanol	12.5	6.94 ± 0.01**
	25	1.78 ± 0.09**
	50	0.15 ± 0.03**
Petroleum ether	12.5	15.16 ± 0.18
	25	9.21 ± 0.05
	50	8.77 ± 0.18
Methanol	12.5	9.78 ± 0.12
	25	7.92 ± 0.08**
	50	6.58 ± 0.05**

$^{\#}P < 0.05$, $^{\#\#}P < 0.01$ *vs* control group; $^{*}P < 0.05$, $^{**}P < 0.01$ *vs* model group.

deduce their chemical structures. As shown in Fig. 2, 17 compounds, namely salicylic acid (**1**), protocatechuic acid (**2**), caffeic acid (**3**), isochlorogenic acid B (**4**), isochlorogenic acid A (**5**), isovanillic acid (**6**), ferulic acid (**7**), 4-hydroxyl-3,5-*O*-dimethoxy benzoic acid (**8**), protocatechuic acid methyl ester (**9**), methyl caffeate (**10**), 3,4-*O*-dicaffeic quinine acid methyl ester (**11**), 3,5-*O*-dicaffeic quinine acid methyl ester (**12**), 3-indole formaldehyde (**13**), 3,6-diisopropylpiperazin-2,5-dione (**14**), caffeine (**15**), scopoletin (**16**), and 4-hydroxy-4-(3-hydroxy-1-butenyl)-3,5,5-trimethyl-2-cyclohexen-1-one (**17**), were identified. Subsequently, all compounds were tested in cytobiological experiments (described in Section 2.4). The dose-effect relationship of each compound was tested using RAW264.7 cell viability (MTT method) as index. As it is indicated in result (data not shown), all compounds were nontoxic (cell viability ≥85%) within the concentration range of 3.125–50 μg/mL, whereas 14 were nontoxic up to 100 μg/mL, and only five were nontoxic up to 200 μg/mL. As a result, the investigation of NF-κB transcription activity was analyzed only at concentrations of 3.125–50 μg/mL. The determination of fluorescence absorbance showed that eight out of 17 compounds inhibited NF-κB transcription to various extents (Fig. 3). Methyl caffeate (compound **10**) was the strongest inhibitor, which indicated that its structure favored binding to the inhibitory site of NF-κB (Table 3). Similarly, most of the above-mentioned above compounds inhibited NO production and were selected for further evaluation. Compound **13** had the fourth strongest activity against NF-κB; However, its effect on NO production was much worse at low and medium (12.5 and 25 μg/mL) concentrations. Along with the consideration of safety, all seven compounds were finally chosen in this step.

3.3. Selection of active compounds

Compounds in trichloromethane fraction were screened for their own activities using the above-mentioned methods. As indicated in Fig. 4 and Table 4, seven compounds (compounds **4**, **5**, **8**, **10**, **11**, **12**, and **17**) significantly inhibited NF-κB expression compared with LPS control ($P < 0.05$). Compounds **4**, **10**, **12**, and **17** effectively inhibited iNOS mRNA expression and NO production, as shown in Fig. 4. Because no standards were available for compounds **12** and **17** as proposed in the literature (Liu et al., 2017; Wang et al., 2017), only compounds **4** and **10** were chosen

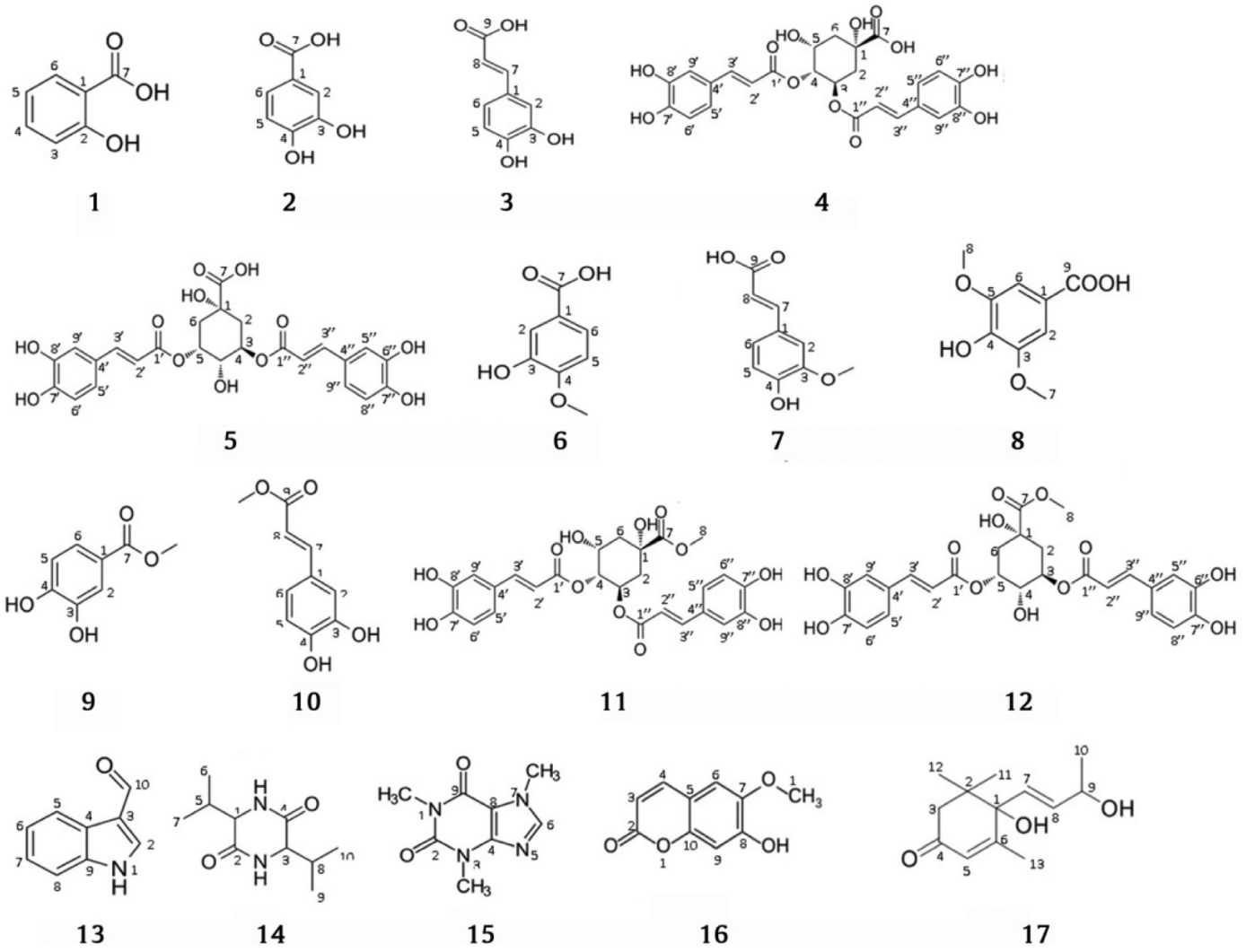

Fig. 2. Chemical structures of compounds **1**–**17**.

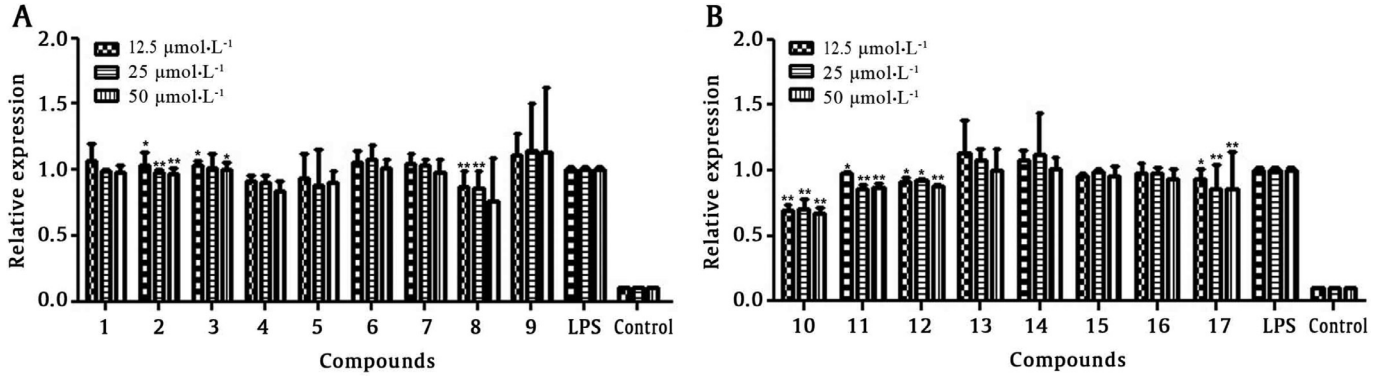

Fig. 3. Effect of each compound (A: coumpounds **1**–**9**; B: coumpounds **10**–**17**) on expression of NF-κB proteins.

as candidates. These findings, along with results of pharmacology experiments, indicated good affiliation and inhibition activities of compounds in the trichloromethane fraction extracted from *J. elongatum*. Trichloromethane was a medium polarity solvent, and soluble compounds in it probably had similarly properties. Such findings also indicated that the traditional way (like decoction) of taking *J. elongatum* may not exert its therapeutic effects to the utmost for the reason of the lack of main active components. Besides, compounds with similar structure (such as compound **4**, **5**, **11**, **12** as well as **9**, **10**, **17**) resulted in much different inhibition rates, judging from the special structure of NF-κB target, changes in structure, location or even configuration of some functional groups would brought about obstacles to their affiliation with target.

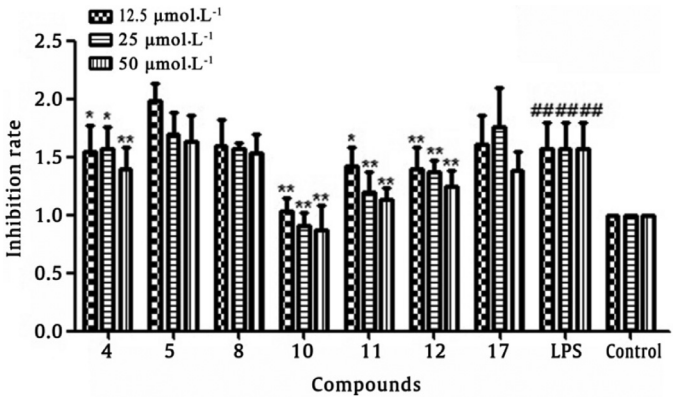

Fig. 4. Inhibition on iNOS mRNA expression by presentative compounds with obvious NF-κB inhibition.

Table 3
Relative expression of NF-κB proteins by each compound (mean ± SD, $n = 3$)

Compounds	Dosage / (μmol•L^{-1})		
	12.5	25	50
1	10.632 ± 1.330	9.931 ± 0.113	9.797 ± 0.587
2	10.397 ± 0.933	9.822 ± 0.207	9.695 ± 0.380
3	10.315 ± 0.397	10.147 ± 1.027	9.953 ± 0.580
4	9.113 ± 0.473	8.988 ± 0.583	8.377 ± 0.733
5	9.317 ± 1.853	8.825 ± 2.703	8.979 ± 0.963
6	10.571 ± 0.833	10.823 ± 1.057	10.162 ± 0.567
7	10.465 ± 0.750	10.353 ± 0.417	9.813 ± 0.910
8	8.719 ± 1.183	8.573 ± 1.287	7.603 ± 3.283
9	11.161 ± 1.633	11.418 ± 3.583	11.275 ± 4.937
10	6.902 ± 0.540	7.011 ± 0.760	6.769 ± 0.447
11	9.785 ± 0.137	8.576 ± 0.337	8.700 ± 0.347
12	9.130 ± 0.357	9.291 ± 0.123	8.758 ± 0.193
13	11.351 ± 2.490	10.786 ± 0.877	10.033 ± 1.640
14	10.736 ± 0.750	11.245 ± 3.163	10.134 ± 0.850
15	9.544 ± 0.210	9.898 ± 0.250	9.585 ± 0.730
16	9.752 ± 0.753	9.811 ± 0.443	9.352 ± 0.743
17	9.375 ± 0.710	8.584 ± 1.887	8.599 ± 2.840
LPS	10.000 ± 0.230	10.000 ± 0.230	10.000 ± 0.230
Control	1.000 ± 0.000	1.000 ± 0.000	1.000 ± 0.000

Table 4
Inhibition on iNOS mRNA relative expression by compounds with obvious NF-κB inhibition (mean ± SD, $n = 3$).

Compounds	Dosages / (μmol•L^{-1})		
	12.5	25	50
10	1.030±0.110	0.907±0.110	0.874±0.210
11	1.423±0.160	1.195±0.170	1.139±0.100
12	1.393±0.190	1.367±0.110	1.249±0.140
17	1.607±0.250	1.762±0.340	1.380±0.170
LPS	1.571±0.230	1.571±0.230	1.571±0.230
control	1.000±0.000	1.000±0.000	1.000±0.000

3.4. Content determination

As shown in Fig. 5 and Table 5, in all 10 batches of samples determined, except compounds **4** and **10**, no obvious peaks of other selected compounds were found in the solution of trichloromethane fraction at therapeutic concentrations. Through careful discussion, all compounds except for **4** and **10** were excluded from the QM candidate list. As a result, compounds **4** and **10** (methyl caffeate and isochlorogenic acid B) were finally chosen as candidates because of their good traceability.

3.5. Pharmacokinetics of candidate QMs in rat plasma

The final step in confirming material basis of *J. amplexicaule* was the evaluation of the metabolism of candidate compounds in the body. As described in Sections 2.7–2.8, a comprehensive process was carried out and pharmacokinetic parameters were determined.

Table 5
Determination of isochlorogenic acid B and methyl caffeate in different batches.

Batches	Weight/g	Isochlorogenic acid B/ (mg·g^{-1})	Methyl caffeate/ (mg·g^{-1})
S1	1.0015	0.6075	0.5651
S2	1.0018	0.6535	0.5807
S3	1.0001	0.5030	0.5187
S4	1.0012	0.5187	0.5294
S5	1.0012	0.5138	0.5322
S6	1.0003	0.5074	0.5245
S7	1.0004	0.4963	0.5017
S8	1.0099	0.5330	0.5029
S9	1.0051	0.5813	0.5186
S10	1.0097	0.6851	0.5965

3.5.1. Optimization of sample pretreatment method

According to previous reports (Chen, Sun, & Bi, 2017; Li, Bi, & Wang, 2012), rat plasma samples were spiked with various types of commonly-used solvents in a series of solvent/plasma ratio to evaluate the ability of each solvent to extract compounds of interest from the complex plasma matrix. Acetonitrile and methanol were used for protein precipitation at solvent/plasma volume ratios of 3:1 and 4:1, respectively. Acetic ether and methyl *t*-butyl ether were used for liquid-liquid extraction. Peak areas of target compounds in standard solution and extracted plasma solution were compared. Acetonitrile was better than methanol for protein precipitation (data not shown), and no significant difference was observed among different ratios of acetonitrile. However, liquid-liquid extraction was better than protein precipitation, which may be because the target compounds were more soluble in the reagent owing to their lower polarities and because their association with plasma proteins cannot be easily avoided by protein precipitation.

3.5.2. Optimization of LC–MS-MS method

Parameters affecting elution and responses of target compounds, such as mobile phase composition, elution program, spray voltage, vaporization temperature, capillary temperature, tube length offset, skimmer offset, and collision energy, were optimized. MS conditions were automatically selected by Tune Master Software (Thermo-Fisher Scientific), and the results indicated that tube length offset and skimmer offset had the strongest influence on responses. Moreover, these influences were much lower (≥20 times) for isochlorogenic acid B than for methyl caffeate within the optimized range. Although responses of isochlorogenic acid B were found in both positive and negative ion modes (*m/z* 517 and 515), the fragment in the negative mode was much lower than that in the positive mode; Therefore, the ion pair at 517/163 was chosen. For chromatography separation, elution time was much shorter (difference of more than 3 min) using acetonitrile than methanol, and the ionization of target compounds was not significantly affected. Furthermore, the addition of formic acid improved peak shape and response. However, no further enhancement was found when formic acid concentration was increased above 0.2%; therefore, the composition of formic acid in the mobile phase was set as 0.1% as described in section 2.9.

3.5.3. Method validation

The optimized LC–MS-MS method underwent a series of tests to validate its reliability to analyze biological samples (Chen et al., 2017; Ramesh, Vadaparthi, & Sukumar, 2017), which included linearity, sensitivity, accuracy, precision, recovery, matrix effect, and stability. The results (data not shown) indicated that

the optimized method had all these values within the acceptable ranges, showing its good suitability for pharmacokinetics analysis.

3.5.4. Pharmacokinetics results

Plasma samples (prepared as described in Section 2.8) were analyzed using the optimized and validated LC–MS-MS method (described in section 2.9). Ratios of peak areas of target compounds and internal standard were interpolated with the calibration curve prepared for the calculation of concentrations of target compounds in the plasma. Moreover, a concentration-time curve was constructed and processed by BAPP2.0 to calculate pharmacokinetic parameters (Fig. 6 and Table 6).

The concentration-time plot for methyl caffeate showed two peaks within a short interval (15 min and 30 min), indicating fast absorption and elimination, whereas at the same time, a part of the already metabolized compound was driven back by enterohepatic circulation, leading to another peak. As shown in Fig. 6, isochlorogenic acid B followed a conventional profile with only one peak and its plasma concentration dropped in a more subtle manner. The above-mentioned curves indicated that these candi-

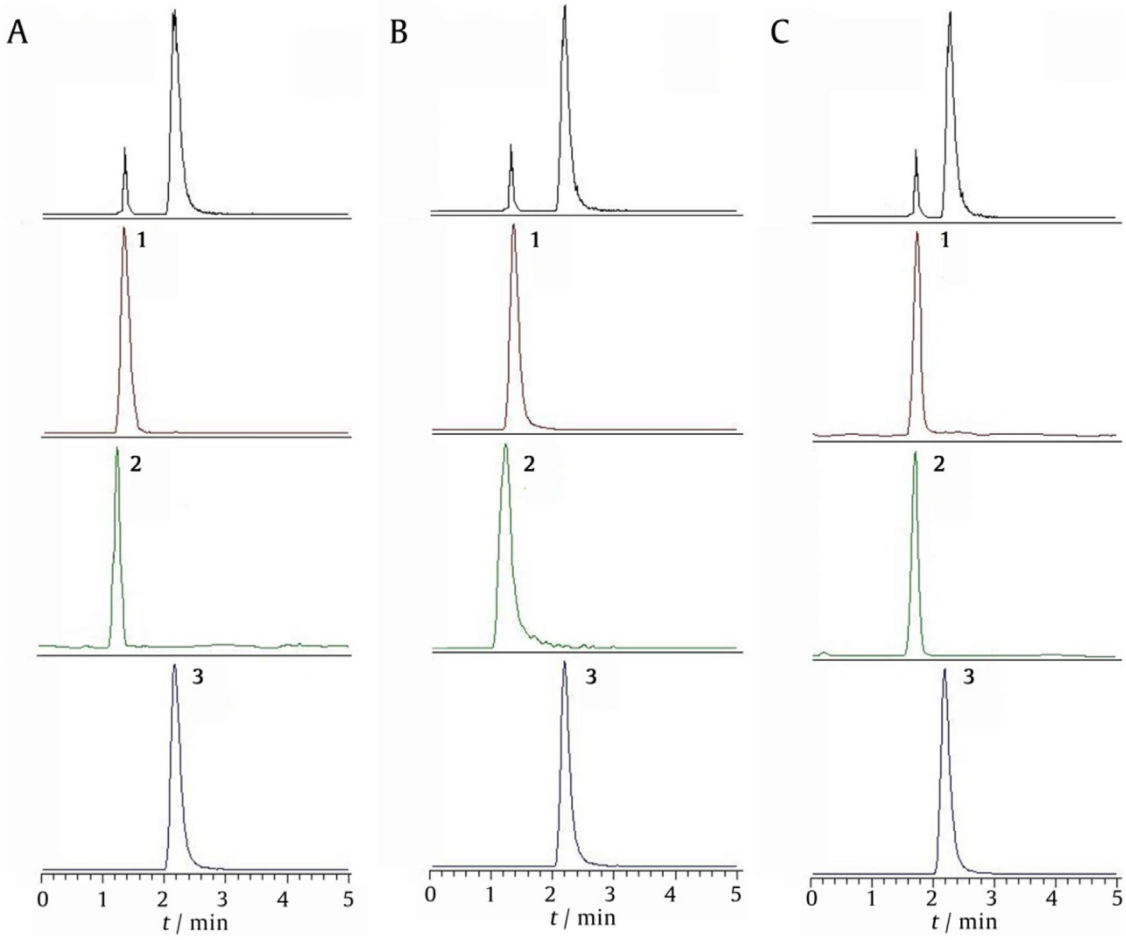

Fig. 5. Total ion current chromatogram of (A) spiked plasma (at concentration of 100 ng/ml), (B) real pharmacokinetic sample (30 min), and (C) herb sample. Compound **1** was methyl caffeate, **2** was isochlorogenic acid B and **3** was IS (piperine).

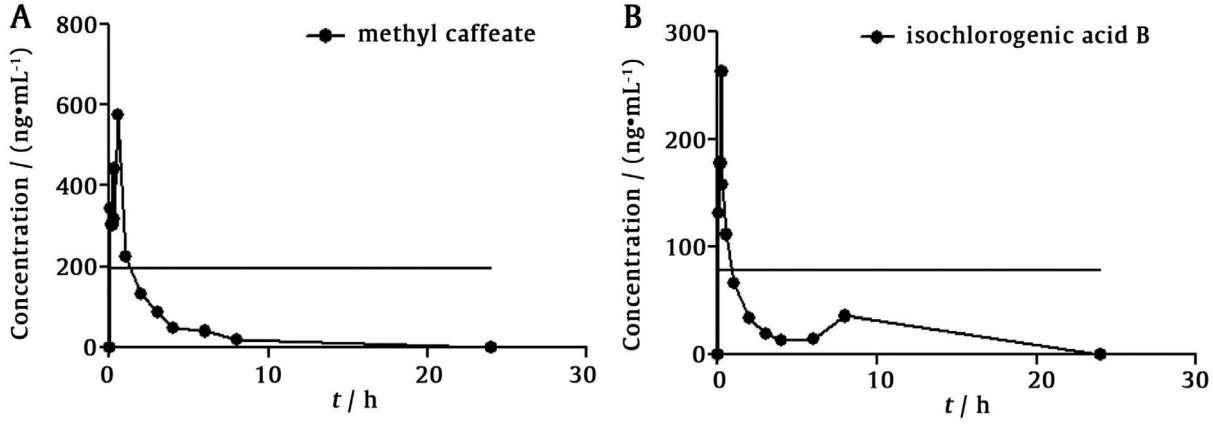

Fig. 6. Plasma concentration-time plot of isochlorogenic acid B (A) and methyl caffeate (B) in rat plasma.

Table 6
Pharmacokinetic parameters of methyl caffeate and isochlorogenic acid B in SD rats (mean ± SD, $n = 6$).

Groups	C_{max} / (ng·mL^{-1})	t_{max}/ h	$t_{1/2}$ / h	MRT/ h	AUC $_{0-\tau}$ / (hng·mL^{-1})	AUC$_{0\sim\infty}$ / (h·ng·m L^{-1})
methyl caffeate	575.35 ± 11.32	0.50	0.45 ± 0.03	2.12	654.85 ± 71.04	667.13 ± 58.27
isochlorogenic acid B	262.03 ± 5.89	0.25	2.03 ± 0.12	5.51	230.10 ± 25.52	334.71 ± 38.31

dates were well absorbed and accumulated in the rat body, and proven to be adequate for the therapeutic effects of *J. elongatum*. For metabolism and elimination, methyl caffeate and isochlorogenic acid B had mean residence times of 2.12 h and 5.51 h, respectively, verifying that their good retention in the body facilitated their interaction with their targets for a desirable period. Based on elimination half-life, which indicates both efficacy and safety of compounds, and an appropriate area under the curve, these candidates showed good bioavailability and safety. The pharmacokinetics results showed good concordance with pharmacology results, indicating that the concentrations of these compounds directly correlated with therapeutic effects of the herb, and results of content determination can be used for efficacy evaluation in the routine quality control of the herb.

4. Conclusion

Through a comprehensive set of tests and validation, the authors found the main active target and material basis for *J. amplexicaule* treating diarrhea and intestinal angina. The results provide a solid foundation for the confirmation of its therapeutic mechanism and integrates previously scattered data. The methods used for the evaluation of pharmacology, mechanism, traceability, and pharmacokinetics were accurate, fast, and reliable. In addition, the main active compounds detected in the trichloromethane fraction indicated that water-based decoction may probably not be rich in such compounds for its higher polarity, and extract prepared with suitable solvent can be a potential alternative in future.

Declaration of Competing Interest

We wish to confirm that there are no known conflicts of interest associated with this publication, and there was no significant financial support for this work that could have influenced its outcome.

Acknowledgments

The authors thank the open topic grant of Guangxi Key Laboratory for TCM Quality Control Research (Gui Zhong Zhong Kai 201402) and Guangxi Institute of Chinese Medicine and Pharmaceutical Science for financial support.

References

Chen, Z., Sun, D. M., & Bi, X. L. (2017). Pharmacokinetic based study on “lagged stimulation” of *Curcumae Longae Rhizoma-Piper nigrum* couplet in their main active components' metabolism using UPLC–MS-MS. *Phytomedicine, 27*, 15–22.

Delporte, C., Backhouse, N., & Erazo, S. (2005). Analgesic–antiinflammatory properties of *Proustia pyrifolia*. *Journal of Ethnopharmacology, 99*, 119–124.

Fredericksen, F., Villalba, M., & Olavarría, V. (2016). Characterization of bovine A20 gene: Expression mediated by NF-κB pathway in MDBK cells infected with bovine viral diarrhea virus-1. *Gene, 581*, 117–129.

Gálvez, J., Crespo, M., & Jiménez, J. (1993). Antidiarrhoeic activity of quercitrin in mice and rats. *Journal of Pharmacy and Pharmacology, 45*, 157–159.

Gao, Z., Yin, J., & Xie, X. (2014). Intracellular signaling mechanisms pharmacological action of *Jasminum amplexicaule* Buch. Ham. (Oleaceae) on gastrointestinal secretion. *Iranian Journal of Pharmaceutical Research, 13*(3), 959–965.

Gupta, M., Mazumder, U., & Sambath, R. (2005). Anti-inflammatory, analgesic and antipyretic effects of methanol extract from *Bauhinia racemosa* stem bark in animal models. *Journal of Ethnopharmacology, 98*, 267–273.

Jahromi, S., Jamshidi, M., & Farazmand, A. (2017). Pharmacological effects of β-*D*-mannuronic acid (M2000) on miR-146a, IRAK1, TRAF6 and NF-kB gene expression, as target molecules in inflammatory reactions. *Pharmacological Reports, 69*, 479–484.

Jia, Q., Su, W., & Peng, W. (2008). Anti-diarrhoea and analgesic activities of the methanol extract and its fractions of *Jasminum amplexicaule* Buch.-Ham. (Oleaceae). *Journal of Ethnopharmacology, 119*, 299–304.

Li, J., Bi, Y. W., & Wang, L. (2012). β-Cyclodextrin enhanced on-line organic solvent field-amplified sample stacking in capillary zone electrophoresis for analysis of ambroxol in human plasma, following liquid–liquid extraction in the 96-well format. *Journal of Pharmaceutical and Biomedical Analysis, 66*, 218–224.

Li, K. Y., Fan, Y. P., & Wang, H. (2015a). Qualitative and quantitative analysis of an alkaloid fraction from *Piper longum* using ultra-high performance liquid chromatography-diode array detector–electrospray ionization mass spectrometry. *Journal of Pharmaceutical and Biomedical Analysis, 109*, 28–35.

Li, Q., Zhai, W., & Jiang, Q. (2015b). Curcumin–piperine mixtures in self-microemulsifying drug delivery system for ulcerative colitis therapy. *International Journal of Pharmacy, 490*, 22–31.

Liu, C., Cheng, Y., & Guo, D. (2017). A new concept on quality marker for quality assessment and process control of Chinese medicines. *Chinese Herbal Medicines, 9*(1), 3–13.

Ramesh, B., Vadaparthi, P. R., & Sukumar, G. (2017). LC–HRMS determination of piperine on rat dried blood spots: A pharmacokinetic study. *Journal of Pharmaceutical Analysis, 6*(1), 18–23.

Shi, J., Zheng, L., & Liu, Z. (2015). Study of pharmacokinetic profiles and characteristics of active components and their metabolites in rat plasma following oral administration of the water extract of *Astragali Radix* using UPLC–MS/MS. *Journal of Ethnopharmacology, 169*, 183–194.

Shi, Z., Song, D., & Li, R. (2014). Identification of effective combinatorial markers for quality standardization of herbal medicines. *Journal of Chromatography A, 1345*, 78–85.

Tanahashi, T., Shimada, A., & Nagakura, N. (1992). Jasamplexosides A, B and C: Novel dimeric and trimeric secoiridoid glucosides from *Jasminum amplexicaule*. *Planta Medica., 58*, 552–555.

Tanahashi, T., Shimada, A., & Takenaka, Y. (1995). Structure elucidation of acylated iridoid glucosides from *Jasminum hemsleyi*. *Chemical and Pharmaceutical Bulletin, 43*(5), 729–733.

Tanahashi, T., Takenaka, Y., & Nagakura, N. (2000). Five secoiridoid glucosides esterified with a cyclopentanoid monoterpene unit from *Jasminum nudiflorum*. *Chemical and Pharmaceutical Bulletin, 48*(8), 1200–1204.

Tanahashi, T., Takenaka, Y., & Nagakura, N. (1999). Three secoiridoid glucosides from *Jasminum nudiflorum*. *Journal of Natural Products, 62*(9), 1311–1315.

Uddin, S., Shilpi, J., & Alam, S. (2005). Antidiarrhoeal activity of the methanol extract of the barks of *Xylocarpus moluccensis* in castor oil- and magnesium sulphate-induced diarrhoea models in mice. *Journal of Ethnopharmacology, 101*, 139–143.

Umamaheswari, M., Asokkumar, K., & Rathidevi, R. (2007). Antiulcer and *in vitro* antioxidant activities of *Jasminum grandiflorum* L. *Journal of Ethnopharmacology, 110*, 464–470.

Wan, L., Sun, Y., & Yu, Q. (2013). *In vitro* permeability analysis, pharmacokinetic and brain distribution study in mice of imperatorin, isoimperatorin and cnidilin in *Radix Angelicae Dahuricae*. *Fitoterapia., 85*, 144–153.

Wang, F., Wang, B., & Wang, L. (2017). Discovery of discriminatory quality control markers for Chinese herbal medicines and related processed products by combination of chromatographic analysis and chemometrics methods: *Radix Scutellariae* as a case study. *Journal of Pharmaceutical and Biomedical Analysis., 138*, 70–79.

Wang, P., Chen, F., & Du, C. (2015). Increased production of BDNF in colonic epithelial cells induced by fecal supernatants from diarrheic IBS patients. *Scientific Reports, 5*, 10121–10129.

Yang, W., Zhang, Y., & Wu, W. (2017). Approaches to establish Q-markers for the quality standards of traditional Chinese medicines. *Acta Pharmaceutica Sinica B, 7*(4), 439–446.

Zhang, Y., Wang, X., & Sha, S. (2012). Berberine increases the expression of NHE3 and AQP4 in sennoside A-induced diarrhoea model. *Fitoterapia, 83*, 1014–1022.